



ISSN NO. 2320-5407

Journal homepage: <http://www.journalijar.com>

INTERNATIONAL JOURNAL  
OF ADVANCED RESEARCH

## RESEARCH ARTICLE

## Effect of Annealing Temperature on Structural and Magnetic Properties of Co-Zn Ferrite Nanoparticles

M.M. Eltabey<sup>1,2</sup>, N.Aboufotoh Ali<sup>3\*</sup>

1. Basic Engineering Science Department, Faculty of Engineering, Menoufiya University, Egypt.
2. Preparatory Year Deanship, Science Department-Physics, Faculty of Medicine, Jazan University, Saudi Arabia.
2. Department of Engineering Physics and Mathematics, Faculty of Engineering, Tanta University, Egypt

### Manuscript Info      Abstract

#### Manuscript History:

Received: 25 April 2014  
Final Accepted: 19 May 2014  
Published Online: June 2014

#### Key words:

Nanoferrites; Annealing;  
Magnetization;  
Superparamagnetism

#### \*Corresponding Author

N.Aboufotoh Ali

Co-Zn ferrite nanoparticles were prepared using co-precipitation method. The effect of annealing temperature on structure and magnetic properties has been investigated. X-ray diffraction (XRD), transmission electron microscope (TEM), infrared spectroscopy (FTIR), and dynamic light scattering (DLS) were used to characterize the structure of the samples. Magnetic hysteresis loops and zero field cooling ZFC curves, in temperature range (5 – 550 K), were measured using vibrating sample magnetometer (VSM) and the values of blocking temperatures ( $T_B$ ) were determined. The results showed that, all the obtained samples were formed in single spinel phase. The crystallinity enhanced and the particle size increased due to the annealing process with temperatures up to 950°C. Although The lattice parameter, magnetization, and blocking temperature showed minimum values at annealing temperature 350°C, the Curie temperature remained almost constant with annealing temperatures.

Copy Right, IJAR, 2014.. All rights reserved.

## 1. Introduction

Polycrystalline spinel ferrites are widely used in many electronic devices. They are preferred because of their high permeability in the radio- frequency (RF) region, high electrical resistivity, mechanical hardness and chemical stability. These types of ferrites are subjects of intense theoretical and experimental investigation due to their remarkable magnetic and electric properties (El-Shabasy M. Et al,1997, Rosales M. I., Et al,1997, Mahmud S.T., Et al,2006). Cobalt ferrite (CoFe<sub>2</sub>O<sub>4</sub>) is a well-known hard magnetic material with high coercivity and moderate magnetization. These properties, along with their great physical and chemical stability, make CoFe<sub>2</sub>O<sub>4</sub> nanoparticles suitable for magnetic recording applications (Skomski R., Et al ,2003). Many efforts have been made to improve the basic properties of these ferrites by substituting or adding various cations of different valence states depending on the applications of interest. Among spinel ferrites, Zn<sup>2+</sup> substituted CoFe<sub>2</sub>O<sub>4</sub> nanoparticles exhibit improved properties such as excellent chemical stability, high corrosion resistivity, magnetocrystalline anisotropy, magnetostriction, and magneto-optical properties (Vaidyanathan.G and Sendhilnathan.S et al, 2008 , AktherHossain. A. K. M., et al, 2008). Various preparation techniques, such as sol-gel pyrolysis method (Lee.J.G., et al, 1998, SonalSinghal, 2010),the microwave hydrothermal method (Kim .C. K., 2001), template-assisted hydrothermal method (He.H.Y., 2011), and combustion technique are used to prepare ferrites nanoparticles. However co-precipitation method is considered as an economical way of producing fine particles (Urcia-Romero S, et al, 2011, Veverka M, et al, 2011). The physical properties of nanoparticles are of current interest due to the size dependent behavior observed in the nano scale and high crystallinity.

In the current study, focus was placed on the Co<sub>0.5</sub>Zn<sub>0.5</sub>Fe<sub>2</sub>O<sub>4</sub> nanoparticles prepared via co-precipitation method. The dependence of the morphology and magnetic properties on annealing temperatures are investigated taking into account that mixed ferrites (Co-Zn) chosen here are highly sensitive to temperature (Vaidyanathan.G, et al, 2011).

## 2. Materials and Methods

Ferrite powder of  $\text{Co}_{0.5}\text{Zn}_{0.5}\text{Fe}_2\text{O}_4$  nanoparticles was prepared by co-precipitation method. A 50 mL of aqueous solution of  $\text{Fe}_2(\text{SO}_4)_3 \cdot 7\text{H}_2\text{O}$ ,  $\text{CoSO}_4 \cdot 7\text{H}_2\text{O}$ , and  $\text{ZnSO}_4 \cdot 7\text{H}_2\text{O}$ , in stoichiometric proportions, was first prepared. It was then mixed with a solution of NaOH, resulting in a dark suspension ( $\text{pH} = 12$ ) of precipitated hydroxides. The mixture was heated and kept at  $80^\circ\text{C}$  on a hotplate, while being steadily stirred, until the precipitates were fully oxidized to form dark brownish spinel ferrites. The product was then filtered and washed several times by distilled water, followed by air-drying at room temperature for 48 h. the powder was sintered at temperatures ( $120, 350, 550, 750$  and  $950^\circ\text{C}$ ) for 2 hours. The heating rate applied was  $4^\circ\text{C}/\text{min}$  up to the sintering temperature.

The obtained powders were analysed by (XRD) with x-ray diffractometer, Philips X'Pert system with Cu-K $\alpha$  radiation ( $\lambda = 0.154056$  nm). Particles shape with microstructural properties were investigated with a transmission electron microscope (JEOL, JEM-1400 Electron Microscope). The particle size distribution was investigated by dynamic laser scattering (DLS), in which the particle size was measured by detecting the Brownian motion of the particles through probing the Doppler frequency shift of a scattered light with respect to the incident light. The diameter detected via dynamic laser scattering is hydrodynamic diameter. Room temperature magnetic measurements were carried out using the Lake-Shore vibrating sample magnetometer (VSM) model 7410. The temperature dependence of magnetization (zero field cooling curves ZCF) was measured using the same VSM in temperature range ( $5\text{-}550\text{K}$ ) and the blocking temperatures  $T_B$  of the investigated samples were determined.

## 3. Results and discussion

### 3.1. X-ray analysis

X-ray diffraction (XRD) patterns for the as prepared and annealed polycrystalline  $\text{Co}_{0.5}\text{Zn}_{0.5}\text{Fe}_2\text{O}_4$  ferrite powders are presented in Figure 1. Comparing the patterns of all the investigated samples with that of standard JCPDS card, a single phase  $\text{Co}_{0.5}\text{Zn}_{0.5}\text{Fe}_2\text{O}_4$  has formed with no extra peaks. At the calcination temperature of  $350^\circ\text{C}$ , the peak corresponding to (222) plane started to appear clearly in the patterns. At  $950^\circ\text{C}$  fully crystallized  $\text{Co}_{0.5}\text{Zn}_{0.5}\text{Fe}_2\text{O}_4$  has formed with sharp peaks indexed as (220), (311), (222), (400), (422), (511), (440) planes of spinel structure. A. M. Rangel et al. reported that (Ana Maria Rangel de FigueiredoTeixeira, et al, 2006), ferrite phase for samples prepared by co-precipitation method was dependent on the heating temperature up to  $200^\circ\text{C}$ . They found that for ferrite samples annealed at  $200^\circ\text{C}$  mostly are in an amorphous phase and that annealed at  $400^\circ\text{C}$  are presented in crystalline phase. In the present work, Figure 1 reveals the presence of the spinel structure for the as prepared  $\text{Co}_{0.5}\text{Zn}_{0.5}\text{Fe}_2\text{O}_4$  sample, and the noticed broadening in the peaks of the as prepared sample could be attributed to the formation of ferrite particles in nano range. The peak width decreases with the increase of annealing temperature which reflects the coarsening of particles. The sizes of the nano particles have been determined using Scherrer's formula from the FWHM of 311 peak and supported by the TEM micrographs. The particle size increases from  $13.8$  nm to  $205.2$  nm with the systematic variation of annealing temperature as shown in Figure 2. The average particle size increases slowly from  $27^\circ\text{C}$  to  $350^\circ\text{C}$ . In the temperature range  $550^\circ\text{C}$ - $750^\circ\text{C}$ , the grain size increases gradually and then for the sintering temperature  $950^\circ\text{C}$ , the size increases sharply.

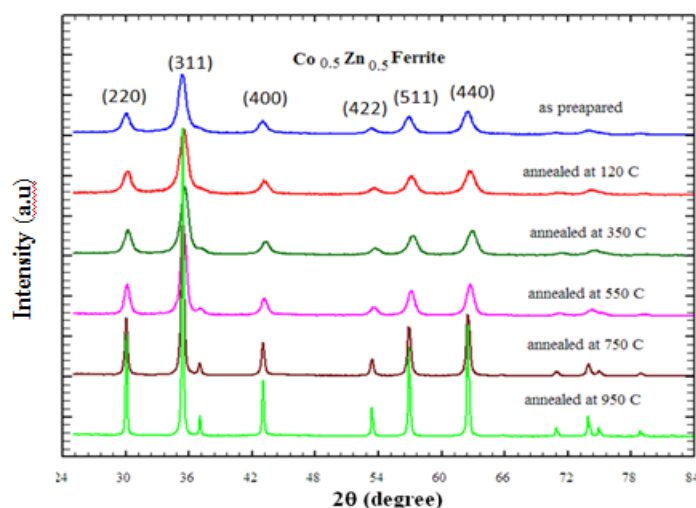
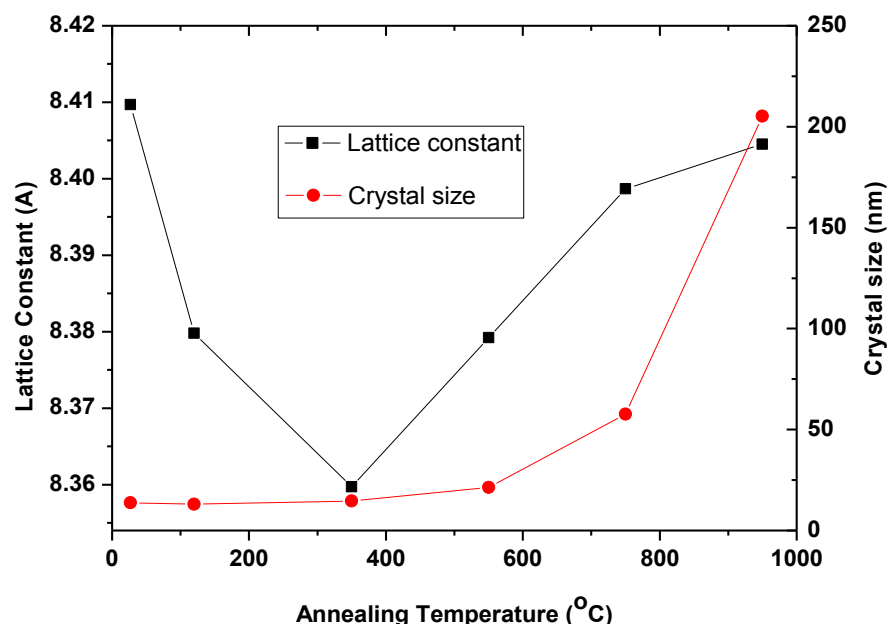


Figure 1. The X-ray diffraction (XRD) patterns for the polycrystalline  $\text{Co}_{0.5}\text{Zn}_{0.5}\text{Fe}_2\text{O}_4$  ferrites powders as prepared and that was annealed at different temperatures ( $120 - 950^\circ\text{C}$ )



**Figure 2. The variation of the particle size of  $\text{Co}_{0.5}\text{Zn}_{0.5}\text{Fe}_2\text{O}_4$  ferrites with different annealing Temperatures (right) and the lattice parameters as a function of the annealing temperatures (left).**

The lattice parameters are plotted as a function of annealing temperature, as shown also in Figure 2. It is observed that the lattice constant 'a' decreases with increasing annealing temperature up to 350 °C then increases with increased temperature up to 950 °C. It is well known that the lattice parameter of ferrite nanoparticles is larger than that in bulk and it decreases as the particle size increases. This observed phenomenon is attributed to the large volume fraction of interface structure (Gleiter.H , 1989) . Also, in case of bulk structure,  $\text{Co}^{2+}$  ions are inverse spinel. They prefer to occupy octahedral sites (B-sites) (Chikazumi.S. et al, 1964). Whereas, many authors reported that, in case of nano structure, nearly 25% to 40% of  $\text{Co}^{2+}$  ions content occupy the tetrahedral sites (A-sites) (Mane.D.R., et al, 2000), SonalSinghal, et al, 2005, SonalSinghal, et al, 2006). As a result of increasing the particle size with increasing the annealing temperature,  $\text{Co}^{2+}$  ions prefer to migrate to B-site. On the other hand, theoretically, the lattice parameter is given by

$$a_{\text{th}} = \frac{8}{3\sqrt{3}} [(r_A + r_O) + \sqrt{3}(r_B + r_O)] \quad (1)$$

Where,  $r_A$  and  $r_B$  are the radii of tetra and octahedral sites respectively and  $r_O$  is the radius of the oxygen ion (1.32 Å) (Sattar, et al, 2005). By the relocation of  $\text{Co}^{2+}$  ions of radius (0.74Å) into B-site the  $\text{Fe}^{3+}$  ions of radius (0.645Å) will occupy A-site, and the end result is the increase of  $r_B$  and decrease of  $r_A$ .

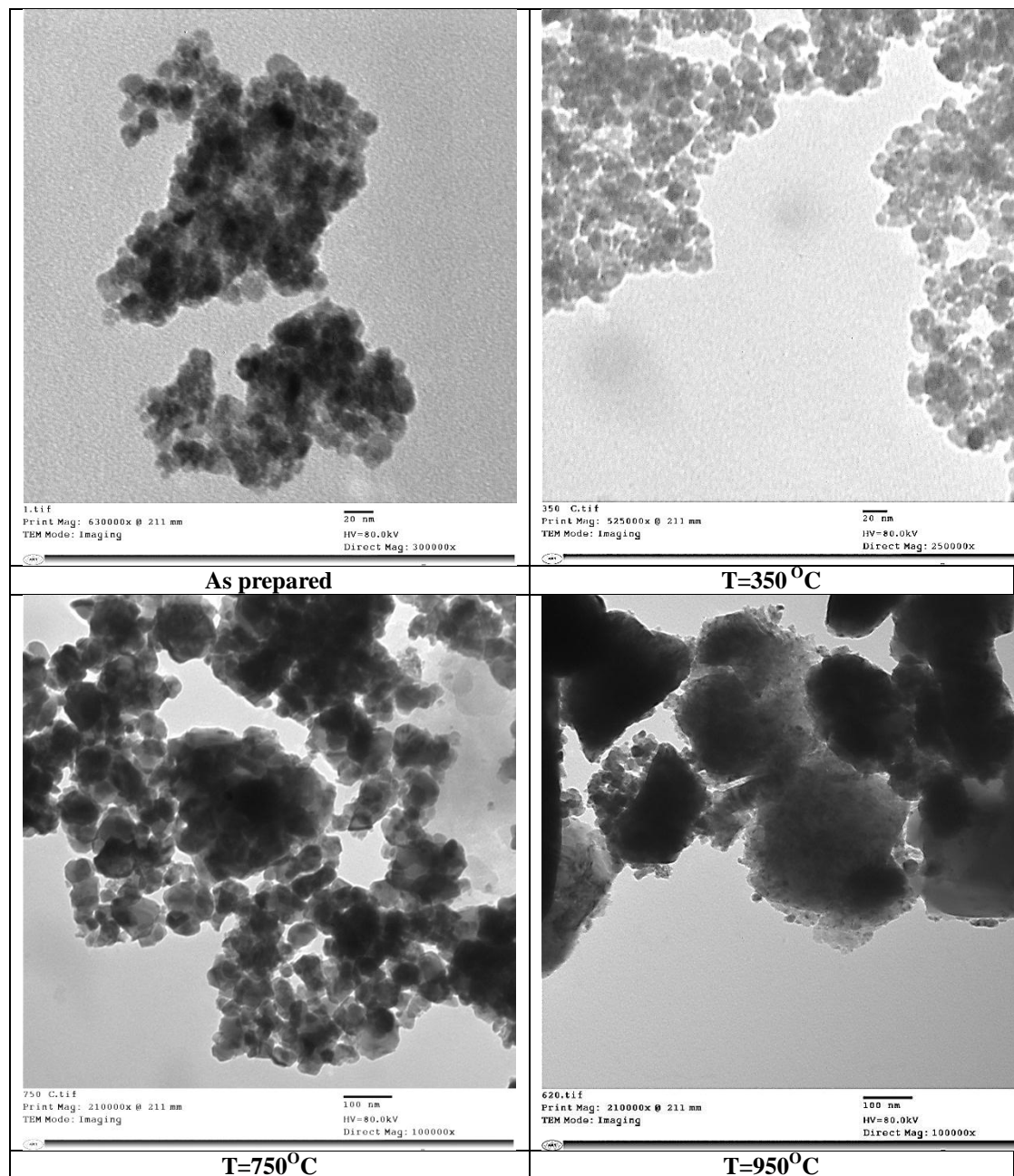
### 3.2. TEM and DLS

Figure 3.shows the TEM micrographs for the as prepared sample and those annealed at 350°C, 750°C and 950°C. The figure illustrates the homogeneity and the spherical shape of the samples up to annealing temperature 350°C. The size of the spherical particles matches the results of XRD analyses. As the annealing temperature increase the average particle size increases due to the crystal growth.

Particle size analysis plays a crucial role in the manufacture of magnetic materials for dielectric applications. In order to investigate the size distribution of magnetic particles, a dynamic laser scattering (DLS) system is used. It is worth to mention that the value of the particle diameter obtained from XRD pattern means the particle core size, whereas the size detected using DLS system refers to a hydrodynamic diameter of particles, this diameter is obtained from comparing a sphere to the translational diffusion coefficient actually measured. A summary of particle size of the samples and their diffusion coefficient are listed in table 1. It is found that the increase of annealing temperature is proportional to the increase in the particle size, while the particle size distribution becomes narrower as the diffusion coefficient reduced.

**Table1. The crystallite size, dynamic laser scattering particle size, and diffusion coefficient for  $\text{Co}_{0.5}\text{Zn}_{0.5}\text{Fe}_2\text{O}_4$  at different annealing temperatures.**

Annealing Temp. (C)	Crystallite size (Å)	DLS Particle size (nm)	Diff. coef. $\times 10^{-12}(\text{m}^2/\text{s})$
27	130	187.3	1.91
120	138	231.7	1.54
350	147	260	1.37
550	214	290	1.23
750	576	380	0.939
950	2052	611	0.586



**Figure 3. The TEM micrographs for four  $\text{Co}_{0.5}\text{Zn}_{0.5}\text{Fe}_2\text{O}_4$  ferrites selected samples; as prepared and those annealed at 350°C, 750°C and 950 °C respectively**

### 3.3. FTIR analyses

IR spectrum is considered an important tool to get information about the structure and the positions of ions in the crystal through the crystal's vibration modes (Sattar.A.A., et al, 2005). In case of bulk structure the two IR fundamental bands  $\nu_1$  and  $\nu_2$  in normal and inverse spinels are due to the tetrahedral and octahedral complexes, while  $\nu_3$  is corresponding to the lattice vibration (Mohan, et al, 1999 ,Ravinder D., 1999). The inset of figure 4 shows the IR spectrum of the investigated samples at different annealing temperatures with three dashed lines corresponding to the three detected bands. No considerable variation in the values of  $\nu_3$  is noticed with different annealing temperature as a result of constant lattice mass, since there isn't any replacement of ions in our study. Variation of both  $\nu_1$  and  $\nu_2$  with annealing temperature is illustrated in figure 4. It is obvious that both tetrahedral and octahedral vibration bands  $\nu_1$  and  $\nu_2$  go to maximum at 350°C and then decay. This could be due to the shrinkage of the lattice at that temperature as observed in the behaviour of lattice parameter before. Where, the band frequency and the bond length are inversely proportional (Sattar.A.A., et al, 2005).

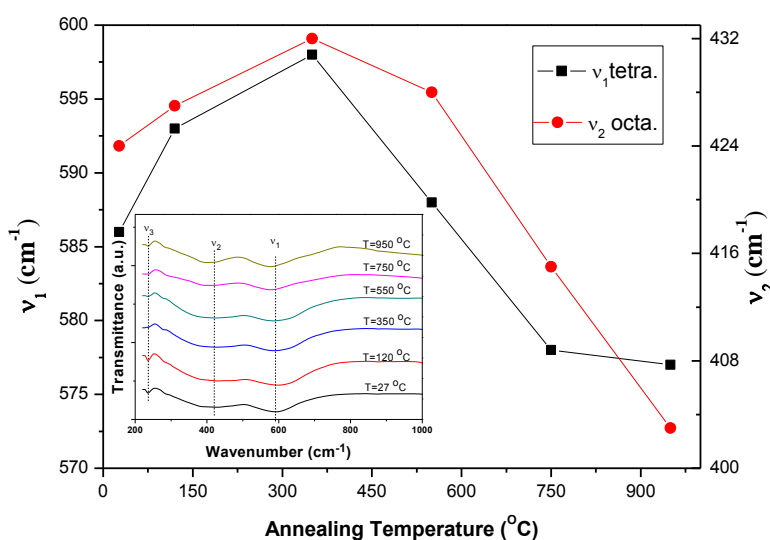


Figure 4. Variation of both  $\nu_1$  and  $\nu_2$  with annealing temperature, the inset is the IR spectrum of the investigated samples at different annealing temperatures.

### 3.4. Magnetic properties

#### 3.4.1 M-H loops

Room temperature M-H loops for annealed samples are shown in figure 5. Super paramagnetic behaviour was detected for as prepared sample as well as samples annealed at 120°C and 350°C due to the small size of the particles of these samples. The values of saturation magnetization  $M_S$  (emu/g) are determined by the extrapolation of magnetization curves with the magnetizing field  $H(T)$ . Inset of figure 5 display the variation of  $M_S$  with annealing temperatures.  $M_S$  shows slight decrease with annealing temperatures till 350°C and sharp rise to temperature 950°C. This behavior could be explained according to the movement of  $\text{Co}^{2+}$  ions with ( $3\mu_B$ ) to B-site and  $\text{Fe}^{3+}$  ions with ( $5\mu_B$ ) to A-site. Taking into account that the magnetization of spinel ferrites is given by  $M=M_B-M_A$ , where  $M_A$  and  $M_B$  are the magnetization of A and B sites respectively (Sattar.A.A., et al, 2005). On the other hand, magnetization and crystallization are enhanced as the particle size increases (Maaz.K., et al, 2007). Therefore, for higher annealing temperatures (>350°C) where the particle size considerably increases, the effect of particle size dominates the relocation of  $\text{Co}^{2+}$  ions.

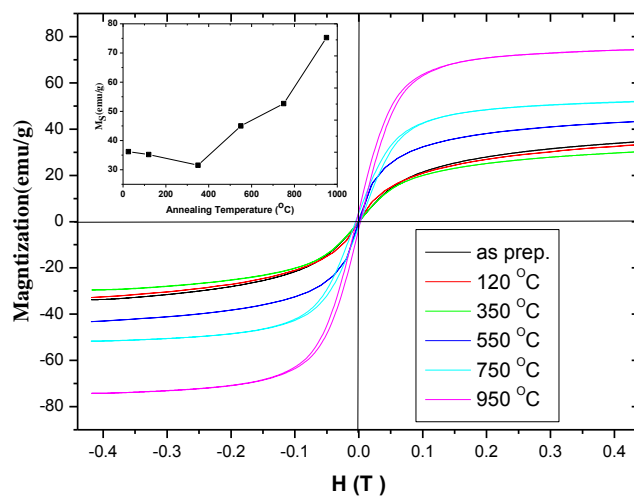


Figure 5. M-H loops for  $\text{Co}_{0.5}\text{Zn}_{0.5}\text{Fe}_2\text{O}_4$  ferrites at different annealing temperatures. Inset is saturation magnetization as a function of annealing temperatures.

### 3.4.2 Temperature dependence of magnetization

Zero field cooling (ZFC) curves are measured at magnetic field  $H=1000\text{Oe}$  in the temperature range from 5 to 570K (figure 6). The peak value of magnetization commonly refers to the blocking temperature ( $T_B$ ) in superparamagnetism.

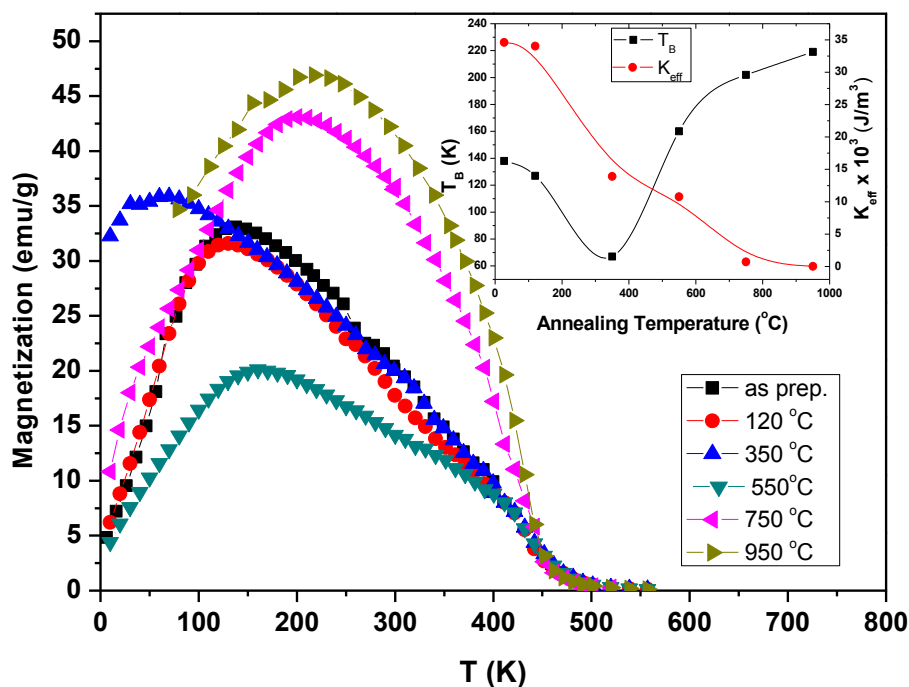


Figure 6. Zero field cooling (ZFC) curves, for  $\text{Co}_{0.5}\text{Zn}_{0.5}\text{Fe}_2\text{O}_4$  ferrites with different annealing temperatures, at magnetic field  $H=1000\text{Oe}$  and T range (5K- 570K). The inset is the blocking temperature and effective magnetic anisotropy constant versus annealing temperatures.

Such a phenomenon is often observed in nanoparticles, each of them is considered as a single magnetic domain. The thermal energy at  $T > T_B$  is sufficient to induce fluctuations in the magnetization direction. Consequently, the expected magnetic-ordered behaviour would not prevail even below the Curie temperature. On the other hand, the observed magnetization would depend on the measurement time  $t_m$  relative to the relaxation time  $\tau$  of thermal fluctuations. The relaxation time  $\tau$  for a single particle is given by (Hamdeh.H.H., et al, 2005),

$$\tau = \tau_0 \exp(K_{\text{eff}}V/k_B T), \quad (2)$$

where a characteristic time  $\tau_0$  is typically  $10^{-9}$  s, and  $k_B T$ ,  $K_{\text{eff}}$ , and  $V$  are, respectively, the thermal energy, the effective magnetic anisotropy constant and the particle volume. The blocking temperature is then,

$$T_B = K_{\text{eff}}V/[k_B \ln(t_m/\tau_0)], \quad (3)$$

with the measuring time  $t_m = \tau$ . By assuming  $t_m/\tau_0 = 10^{11}$  in a typical magnetization measurement, leading to,

$$T_B = K_{\text{eff}}V/25k_B. \quad (4)$$

Variation of  $T_B$  and effective magnetic anisotropy constant  $K_{\text{eff}}$  with annealing temperatures is represented as an inset of figure 6.  $T_B$  reaches its minimum at 350 °C where  $K_{\text{eff}}$  (derived using equation (4)) reduced dramatically with annealing temperatures. Since  $\text{Co}^{2+}$  ions migrate from A-sites with small radius to B-sites with larger radius, both the internal stress and effective anisotropy constant is reduced. This leads to reduction of  $T_B$  at 350°C as the effect of particle size in this range is not considerable. The enhancement of  $T_B$  values at annealing temperatures ( $> 350^\circ\text{C}$ ) indicates that; the effect of particle size enlargement overcomes decreasing the value of  $K_{\text{eff}}$  with increasing the annealing temperature.

When the temperature exceeded  $T_B$ , the value of magnetization approaches zero approximately at 500K for all samples (figure 6). This behavior reveals that the Curie temperature  $T_C$  for all samples is almost constant. According to ion pair model, the main factor affects the value of  $T_C$  is the A-B interaction (Eltabey.M.M., et al, 2011). The common value of  $T_C$ , especially for the samples which are annealed above 350 °C, could be attributed to the struggle between two factors; the relocation of  $\text{Fe}^{3+}$  ions as discussed before, leads to amplify Fe-Fe interaction in A and B-sites and hence increasing the value of  $T_C$ . On the other hand, the moments separated by large distances due the enhancement of the lattice parameter then the A-B interaction get weaker and hence reduce the value of  $T_C$ .

#### 4. Conclusion

Nano-sized particles of  $\text{Co}_{0.5}\text{Zn}_{0.5}\text{Fe}_2\text{O}_4$  were synthesized using co-precipitation method and the obtained powders were annealed at different temperatures. The annealing process improved the crystallization due to particle size enlargement. The lattice parameter, magnetization, and blocking temperature showed minimum values at annealing temperature 350°C, whereas, Curie temperature remained almost constant with annealing temperatures. The results were discussed in the light of two sub-lattices structure and ion pair model.

#### References:

**Akther Hossain. A. K. M., Tabata. H, and T. Kawai. (2008).** Magnetoresistive properties of  $\text{Zn}_{1-x}\text{Co}_x\text{Fe}_2\text{O}_4$  ferrites. *J. Magn. Magn. Mater.* 320:1157–1162.

**Ana Maria Rangel de Figueiredo Teixeira, Tsuneharu Ogasawara, Maria Cecília de Souza Nóbrega. (2006).** Investigation of sintered cobalt-zinc ferrite synthesized by coprecipitation at different temperatures: a relation between microstructure and hysteresis curves. *Materials Research.* 9 No. 3: 257-262.

**Chikazumi. S. (1964).** *Physics of magnetism, John Wiley & Sons, Inc., New York.*

**El-Shabasy M. (1997).** DC electrical properties of Zn-Ni ferrites. *J. Magn. Magn. Mater.* 172:188.

**Eltabey. M.M., El-Shokrofy. K.M., Gharbia. S.A. (2011).** “Enhancement of the magnetic properties of Ni–Cu–Zn ferrites by the non-magnetic Al<sup>3+</sup> ions substitution” *Journal of Alloys and Compounds* 509 :2473–2477

**Gleiter. H. (1989)** “Nanocrystalline Materials : Review” *Prog. Mater. Sci.* 33, 223.

**Mane.D.R.,Devatwal.U.N., Jadhav.K.M. (2000).** “Structural and magnetic properties of aluminium and chromium co-substituted cobalt ferrite” *Materials Letters* 44 :91–95.

**Hamdeh.H.H.,Hikal.W.M., Taher. S.M., Ho. J.C., Thuy. N.P., Quy. O.K.(2005).** “Mössbauer evaluation of cobalt ferrite nanoparticles synthesized by forced hydrolysis” *J. Appl. Phys.* 97, 064310

**He.H.Y. (2011).**Magnetic Properties of  $\text{Co}_{0.5}\text{Zn}_{0.5}\text{Fe}_2\text{O}_4$  Nanoparticles Synthesized by a Template-Assisted Hydrothermal Method” *Journal of Nanotechnology* .Article ID 182543.

**Kim .C. K., Lee .J. H., Katoh.S, Murakami.R, and Yoshimura.M. (2001).**Synthesis of Co-Co—Zn and Ni—Zn ferrite powders by the microwave-hydrothermal method. *Materials Research Bulletin*.vol. 36.no. 12 :2241–2250.

**Lee.J. G., Minlee.H., Kim.C.S. (1998).**Magnetic properties of  $\text{CoFe}_2\text{O}_4$  powders and thin films grown by a sol-gel method. *J. Magn. Mater.* 90 :177.

**Maaz.K.,ArifMumtaz, Hasan. S. K., Abdullah Ceylan (2007).** “Synthesis and magnetic properties of cobalt ferrite ( $\text{CoFe}_2\text{O}_4$ ) nanoparticles prepared by wet chemical route”*Journal of magnetism and magnetic materials*, V308, 2 :289-295.

**Mahmud S.T., Akther Hossain A.K. M., Abdul Hakim A K M., Seki M., Kawai T. and Tabata H. (2006).**Influence of microstructure on the complex permeability of spinel type Ni–Zn ferrite. *J. Magn. Mater.*305 : 269–274.

**Mane.D.R.,Devatwal. U.N., Jadhav. K.M., (2000).** “Structural and magnetic properties of aluminium and chromium co-substituted cobalt ferrite” *Materials Letters* 44 :91–95.

**Mohan, K and Venudhar (1999).**“Far-infrared Spectra of Lithium–cobalt Mixed Ferrites”*J. Mater. Sci. Lett.* 18 :13-16.

**Ravinder D. (1999).**“Far-infrared spectral studies of mixed lithium-zinc ferrites ” *J. Mater.Lett.*, 40 :205-208.

**Rosales M. I., Amano E., Cuautle M. P. and Valenzuela R. (1997).** Impedance spectroscopy studies of Ni–Zn ferrites. *Materials Science and Engineering, B* 49 :221.

**Sattar, El-Sayed.H.M., El-Tabey.M.M. (2005).**“The effect of Al-substitution on structure and electrical properties of Mn-Ni-Zn ferrites” *J. Mater. Sci.* 40 (18) :4873–4879.

**Sattar.A.A., El-Sayed. H.M., El-Shokrofy.K.M., El-Tabey.M.M. (2005).** “Improvement of the Magnetic Properties of Mn-Ni-Zn Ferrite by the Non-magnetic Al-Ion Substitution” *J. Appl. Sci.* 5 (1) :162–168.

**Skomski R. (2003).**Nanomagnetics. *J. Phys.: Condens. Matter.* 15: R1-R56.

**SonalSinghal, Barthwalb. S.K., Kailash Chandra (2006).** “XRD, magnetic and Mössbauer spectral studies of nano size aluminum substituted cobalt ferrites ( $\text{CoAl}_x\text{Fe}_{2-x}\text{O}_4$ )” *Journal of Magnetism and Magnetic Materials* 306 :233–240

**SonalSinghal, Singh.J.,Barthwal.S.K., Chandra.K (2005).** “Preparation and characterization of nanosize nickel-substituted cobalt ferrites ( $\text{Co}_{1-x}\text{Ni}_x\text{Fe}_2\text{O}_4$ ) ” *Journal of Solid State Chemistry* 178 :3183–3189.

**SonalSinghal, TseringNamgyal, Sandeep Bansal, Kailash Chandra. (2010).** Effect of Zn Substitution on the Magnetic Properties of Cobalt Ferrite Nano Particles Prepared Via Sol Gel Route. *J. Electromagnetic Analysis & Applications.* 2: 376-381.

**Urcia-Romero S, Perales Pérez O, Uwakweh O. N. C, Osorio C, Radovan H. A. (2011)** .Tuning of magnetic properties in Co—Zn ferrite nanocrystals synthesized by a size controlled co-precipitation method. *Journal of Applied Physics*, 109. Issue 7: 07B512-07B512-3.



**Vaidyanathan.G and Sendhilnathan.S (2008).**Characterization of  $\text{Co}_{1-x}\text{Zn}_x\text{Fe}_2\text{O}_4$  nanoparticles synthesized by co-precipitation method. *Physica B*. vol. 403.no. 13-16: 2157–2167.

**Vaidyanathan.G, Sendhilnathanb.S, Arulmurugan.R.(2011).** Structure and magnetic properties of  $\text{Co}_{1-x}\text{Zn}_x\text{Fe}_2\text{O}_4$  nanoparticles by co-precipitation method. *J. Magn. Magn.Mater.*313 :293–299.

**Veverka M, Jiráček Z, Kaman O, Knížek K, Maryško M, Pollert E, Závěta K, Lančok A, Dlouhá M, Vratislav S. (2011).** Distribution of cations in nanosize and bulk Co–Zn ferrite. *Nanotechnology*, Aug 26; 22(34) :345701.